Applied Geography 51 (2014) 108–117

Contents lists available at ScienceDirect

Applied Geography

journal homepage: www.elsevier.com/locate/apgeog

Wildfire hazard in the home ignition zone: An object-oriented analysis integrating LiDAR and VHR satellite imagery

Rutherford V. Platt*

Gettysburg College, 300 North Washington Street, Gettysburg, PA 17325, USA

Keywords:
Wildland–urban interface
Home ignition zone
Wildfire
Object-oriented
GIS and remote sensing
Hazard

A B S T R A C T

Many spatially explicit studies of wildfire hazard focus on the wildland–urban interface (WUI), the area where natural vegetation intersects or mixes with structures. However, research suggests that the characteristics of a small portion of the WUI, the home ignition zone, largely determine potential for ignition from wildfire. The home ignition zone (HIZ) is the area that includes a structure and its surroundings out to 30–60 m. The primary goal of this study is to develop metrics to characterize land cover, burned area, and topography in the HIZ. Pre-fire metrics (i.e. related to land cover and topography) help identify relatively hazardous individual HIZes or neighborhoods of HIZes. Post-fire metrics can be used to assess the burned area across land cover types, inside and outside the HIZ. To calculate the HIZ metrics, multiple data sources (e.g. high resolution 8-band multispectral imagery and LiDAR point clouds) were integrated using an object-oriented image analysis. The setting for the study is the Fourmile Canyon area west of Boulder, Colorado, a data-rich area which experienced a large, destructive wildfire in September 2010. The land cover, burn area, and topography metrics were successfully and accurately calculated and then pre-fire metrics were combined into a simple HIZ hazard index. HIZ characteristics broadly mirror the characteristics of the WUI within the fire perimeter as a whole, though the HIZ on average contains more bare and less forest land, has more widely spaced canopies, and experienced less burning during the fire. The HIZ hazard index values were spatially heterogeneous, but with several distinct high and low hazard clusters. The methods described in this study, paired with *in situ* data collection, can be applied to other areas to inform hazard mitigation plans.

Introduction

As a complex human-environmental system of increasing importance, wildfire is a natural topic of applied geographical research, which has long focused on the physical processes, spatial distribution, and mitigation of hazards (Montz & Tobin, 2011). The severity and destructiveness of wildfires in the western United States has increased in the last 20 years due to factors such as drought, the buildup of hazardous fuels in some ecosystems, and the decentralization of populations into fire-prone areas of the west and southwest (Hammer, Stewart, & Radeloff, 2009; Mell, Manzello, Maranghides, Butry, & Rehm, 2010; National Interagency Fire Center, 2009). In 2012, 67,774 wildland fires were reported across the United States totaling over 3.6 million ha (National Interagency Fire Center, 2012). In Colorado alone, 595 properties were destroyed in two fires: the High Park Fire west of Fort Collins, and the Waldo Canyon Fire, in and to the west of Colorado Springs. Wildfires also devastated communities of Oklahoma, Idaho, Washington, and California.

Many spatially explicit assessments have been conducted to evaluate the effects of or potential for wildfire. Typically these assessments are focused on the wildland–urban interface (WUI), the area where natural vegetation intersects or mixes with structures. The extent of the WUI is highly dependent on the specific definition used (Platt, 2010), but according to one estimate covered 9% of land area and 39% of all structures in the United States (Radeloff et al. 2005). Traditionally defined, the 'hazard' is the nature of an event that is likely to cause harm, while 'risk' is the probability of the event (Montz & Tobin, 2011). Studies of wildfire *risk* in the WUI often evaluate the statistical relationship between ignition and WUI characteristics such as building density and forest fragmentation (Chas-Amil, Touza, & Garcia-Martinez, 2013), distance to urban area and temperature (Badia, Serra, & Modugno, 2011), anthropogenic land use (Guglietta, Conedera, Mazzoleni, & Ricotta, 2011), and road

* Tel.: +1 717 337 6078; fax: +1 717 337 6252.
E-mail addresses: rplatt@gettysburg.edu, rudplatt@hotmail.com.

http://dx.doi.org/10.1016/j.apgeog.2014.03.011
0143-6228/

networks (Castillo, 2012; Lampin-Maillet, 2011; Narayanaraj & Wimberly, 2012). In contrast, studies of wildfire *hazard* in the WUI typically model potential wildfire intensity or exposure based on factors such as vegetation, topography, and housing density (for example, see Bar Massada, Radeloff, Stewart, & Hawbaker, 2009; Herrero-Corral, Jappiot, Bouillon, & Long-Fournel, 2012; Lein & Stump, 2009; Theobald & Romme, 2007). Such landscape-scale assessments of risk and hazard allow analysts to make broad spatial comparisons, but have a major limitation: they cannot be reliably applied to individual structures or neighborhoods. This is primarily because wildfire hazard to structures is to a large degree determined by local rather than landscape factors (Cohen, 2008).

Modeling and experimental research have shown that a small subset of the WUI, the area within 30–60 m of structures, largely determines potential for structure ignition from wildfire (Cohen, 2000, 2001; Cohen & Butler, 1998). This area is known as the known as the home ignition zone (HIZ). Specifically, potential for ignition is primarily a function of wildfire behavior within the HIZ and building characteristics that can make structures more resistant to firebrands and heat transfer (Ager, Vaillant, & Finney, 2010; Cohen, 1991; Cohen & Butler, 1998). The National Fire Protection Association (2008) and Federal Emergency Management Agency (2008) have translated these findings and others into standards for reducing ignition hazards. The NFPA and FEMA recommendations are broadly in alignment, though differ in some details. Generally, builders or homeowners are advised to remove all trees, firewood, and dead branches immediately adjacent to a structure. Within close proximity to the structure, homeowners are advised to thin trees so that canopies are separated, to maximize paved and gravel areas, and to remove other fuel sources (slash piles, wood piles, propane tanks). Fine scale variations in topography influence fire spread, for example by modifying wind speed/direction and fuel moisture (Holden & Jolly, 2011). If structures are located on dangerous topographical features – for example steep slopes, saddles, ridges, or narrow canyons – homeowners are encouraged to extend protection measures even further (e.g. require more aggressive thinning/spacing in HIZ, Slack, 2000). Finally, homeowners are advised to use construction design and materials appropriate for fire-prone areas (e.g. firewise roofing and siding, vents, eaves, soffits, decks, windows, and doors).

Despite the importance of local factors to wildfire hazard, only a small number of spatially explicit studies in the peer reviewed literature focus on the HIZ. One study of an Australian wildfire quantified factors such as cover of trees/shrubs within 40 m, whether trees/shrubs were remnant or planted, the upwind distance from houses to trees/shrubs, the upwind distance from houses to prescribed burns conducted within 5 years, and the number of structures within 40 m of houses (Gibbons et al., 2012). Studies of wildfire in southern California (Syphard, Keeley, Bar Massada, Brennan, & Radeloff, 2012) and Alberta, Canada (Beverly, Bothwell, Conner, & Herd, 2010) quantified the spatial morphology of housing and its relationship to ignition exposure. Finally, a study of the Hayman Fire in Colorado quantified factors like slope, proximity to fire station, vegetation density, and area of defensible space surrounding structures (Bhandary & Muller, 2009). These studies focus on local scales (e.g. individual structures and neighborhoods), and typically use basic variables describing land cover (typically limited to percent vegetation cover) and topography (typically limited to slope and aspect). A possible reason that spatially explicit studies of the HIZ are so sparse is due to the expense or lack of availability of LiDAR data and very high resolution (VHR) multispectral imagery. To identify structures or neighborhoods characterized by potentially hazardous HIZes, there is a need to develop a set of sophisticated, accurate metrics that leverage these data sources.

The first and primary goal of this study is to develop methods to automatically extract information that is useful in assessing relative hazard in the HIZ and the wider landscape. Building on existing literature, the methods exploit data sources such as LiDAR and VHR multispectral imagery, as well as emerging methods such as object-oriented image analysis. More specifically, the goal is to develop metrics related to pre-fire land cover, burned area, and topography. By characterizing the pre-fire land cover and topography, relatively hazardous individual HIZes or neighborhoods of HIZes can be identified. A simple HIZ hazard index comprising the pre-fire metrics was constructed to facilitate broad comparisons. By characterizing the HIZ post-fire, preliminary assessment of the burned area can be conducted and compared to the wider landscape. Ideally the metrics and index described here would be integrated into broader mitigation plans that also include data collection pre- and post-fire. The second goal is to apply the methods to a specific data rich area: the Fourmile Canyon west of Boulder Colorado, the site of a highly destructive fire in September 2010.

While it is tempting to evaluate the statistical relationship between HIZ characteristics and structure survival, such analyses are be problematic for a number of reasons and will not be part of this study. First and foremost, many factors associated with structure loss are often unknown prior to a fire, and difficult to find out afterwards. For example, building materials typically must be identified *in situ* and cannot be reliably identified through GIS/remote sensing. Furthermore, fire suppression and defensive actions taken by homeowners are generally not accounted for in statistical models (Maranghides & Mell, 2009). Finally, firebrand and flame exposure for each individual structure are difficult to determine and the statistical reliability is questionable given the wide variety of conditions and the relatively small number of structure losses (Cohen, personal correspondence, 9/23/2011). Therefore, this study is focused on accurate characterization of the HIZ rather than statistical relationships to structure survival per se.

Methods

Overview

For the purposes of this study, the HIZ was defined as a 30 m buffer from the building footprints (the conservative end of the 30–60 m range identified by Cohen, 2001). The primary data sources for the analysis are WorldView-2 Imagery, LiDAR, and building footprints created by Boulder County GIS (Table 1). Using these primary data sources, the HIZ for each structure was characterized in terms of pre-fire land cover, burned area, and topography (Table 2) and calculated a simple HIZ Hazard index from the metrics.

Study area

Located west of Boulder Colorado, the Fourmile Canyon area is a classic WUI landscape with a complex land ownership pattern that includes private, BLM, USDA Forest Service, and Colorado State land (Fig. 1). It is also the site of the Fourmile Fire which burned 2500 ha and destroyed 168 homes (out of 474 homes and 848 other structures within the burn perimeter) from September 6th–16th, 2010 (Graham et al., 2012, 110 pp.). The housing density within the burn perimeter averaged 1 house per 5 acres, but is considerably more than this along canyon roads. Ranging from 5361 to 9348 m in elevation, the burn perimeter is situated in the montane zone of the Colorado Front Range. The lowest elevations of the montane zone are dominated by open park-like stands of ponderosa pine (*Pinus ponderosa*), mixed Rocky Mountain juniper (*Juniperus scopulorum*) on south facing slopes and with Douglas fir (*Pseudotsuga menziesii*)

Table 1
Primary data sources for deriving pre-fire land cover and burned area in the HIZ.

WorldView-2 Imagery		
Source	DigitalGlobe (http://www.digitalglobe.com/about-us/content-collection#worldview-2)	
Dates	June 10, 2010 and Sept 10, 2010	
Resolution (GSD)	0.5 m (RGB) and 2 m (8-band multispectral)	
Bands	Coastal	400–450 nm
	Blue	450–510 nm
	Green	510–580 nm
	Yellow	585–625 nm
	Red	630–690 nm
	Red Edge	705–745 nm
	Near-IR1	770–895 nm
	Near-IR2	860–1040 nm
LiDAR		
Source	Boulder Creek Critical Zone Observatory (http://criticalzone.org/boulder/)	
Date	August, 2010	
Sensor	Optech GEMINI Airborne Laser Terrain Mapper (ALTM)	
Aircraft	Piper PA-31 Chieftain twin engine	
Point Density	10.28 p/m^2	
Laser PRF	100 kHz	
Flight Altitude	600 m	
Scan angle	±14°	
Horizontal accuracy	~11 cm	
Vertical accuracy	5–30 cm	
Building footprints of 1322 structures		
Source	Boulder County GIS (http://www.bouldercounty.org/gov/data/pages/gisdldata.aspx)	
Date	October 2010	
Method	Manual digitization	

Table 2
Metrics for characterizing the HIZ, including the method and data sources.

Category	Metric	Method	Main data sources
Pre-fire land cover	Percent cover	Forest, grass, bare as a % of total area	Land cover objects
	Forest contiguity	Average nearest neighbor distance between forest polygons	Land cover objects
	Adjacency of canopy to structure	Evaluate if structure polygons intersect or adjoin forest polygons	Land cover objects, building footprints
	Predominance of ladder fuels	% of LiDAR Returns from 1 to 3 m from surface	LiDAR point cloud and DEM
Burned area	Percent burned cover	Burned forest and burned grass as a % of total area	Land cover objects
	Structure survival (yes/no)	Logistic Regression	Building footprints, WorldView-2 imagery, percent cover, percent burned cover
Topography	Slope	Average within HIZ in degrees	LiDAR point cloud and DEM
	Northness	Cosine of the aspect	LiDAR point cloud and DEM
	Landform class (V-shaped canyon, ridge top, saddle, chimney)	Topographic Position Index (Jenness, 2006)	LiDAR point cloud and DEM
	Exposure	Aspect ratio of structure relative to the downhill direction within HIZ (FEMA, 2008; Slack, 2000)	Building footprints, LiDAR point cloud and DEM

on north-facing slopes. In contrast, the upper elevations of the montane zone are dominated by dense mixed stands of Douglas fir and ponderosa pine, with a thick understory of shrubs and grasses. Historically, the lower elevations of the montane zone were dominated by surface fires at intervals of 10–40 years, while the upper montane zone was characterized by a mixture of surface fires and stand replacing fires (Veblen, Kitzberger, & Donnegan, 2000). At the time of the fire, the fine dead fuels from ponderosa pine, rocky mountain juniper, and Douglas fir were very dry due to dry and warm weather in August 2010 (Graham et al., 2012, 110 pp.). Live fuel moistures were at or slightly below normal. According to the Sugarloaf RAWS weather station, winds were blowing downslope from 16 to 24 kph, with gusts up to 66 kph the morning of September 6th.

The Fourmile Canyon Fire Findings report (Graham et al., 2012, 110 pp.) stated that most of the fire growth (93% of the total area) and most home destruction took place during short bursts of extreme fire conditions on September 6th. During this time, the structure protection capability of local fire departments was overwhelmed (Graham et al., 2012, 110 pp.). While the WUI as a whole was experiencing extreme fire conditions, the HIZ often experienced lower intensity surface fires. Indeed, the study found that 83% of destroyed homes were associated with low-intensity fire, as estimated by the degree of consumed vegetation surrounding a home. This is consistent with previous studies that show that home destruction mostly occurs with low and moderate intensity burning, as urban structures such as roads act as a firebreak to disrupt the most intense fire behavior (Cohen & Stratton, 2008). Since many houses in the WUI are widely spaced, the fire generally did not travel directly from house to house and the structures themselves did not significantly promote wildfire growth. By visually assessing remotely sensed imagery, the authors identified a topographic effect where north-facing slopes and canyon bottoms were less affected by fire, and where steep southerly slopes were more affected. However, the authors found no evidence that the 240 ha of fuel treatments (~10% of the total burned area) affected fire behavior. Many factors made it difficult to make judgments about treatment effectiveness, including the shear variety of prescriptions, the lack of prescribed fire, and the many remaining piles of slash in treatment areas. While fire protection was clearly not effective for structures that were destroyed, it was difficult to evaluate the role of fire protection in saving the structures that survived. Mountain Pine Beetle was likely not a factor, as the Fourmile Fire area had only small patches of lodgepole pine and ponderosa pine trees attacked or killed by Mountain Pine Beetle (*Dendroctonus ponderosae*).

The Fourmile Canyon Fire Findings report was based on post-fire *in situ* observations, interviews, and qualitative interpretation of imagery. In contrast, this study focuses on automated extraction of quantitative information from remotely sensed imagery and other available GIS data.

HIZ metrics: pre-fire land cover

Fine-scale information about vegetation and fuel is needed to reliably assess wildfire hazard (Ottmar, Blake, & Crolly, 2012). In this

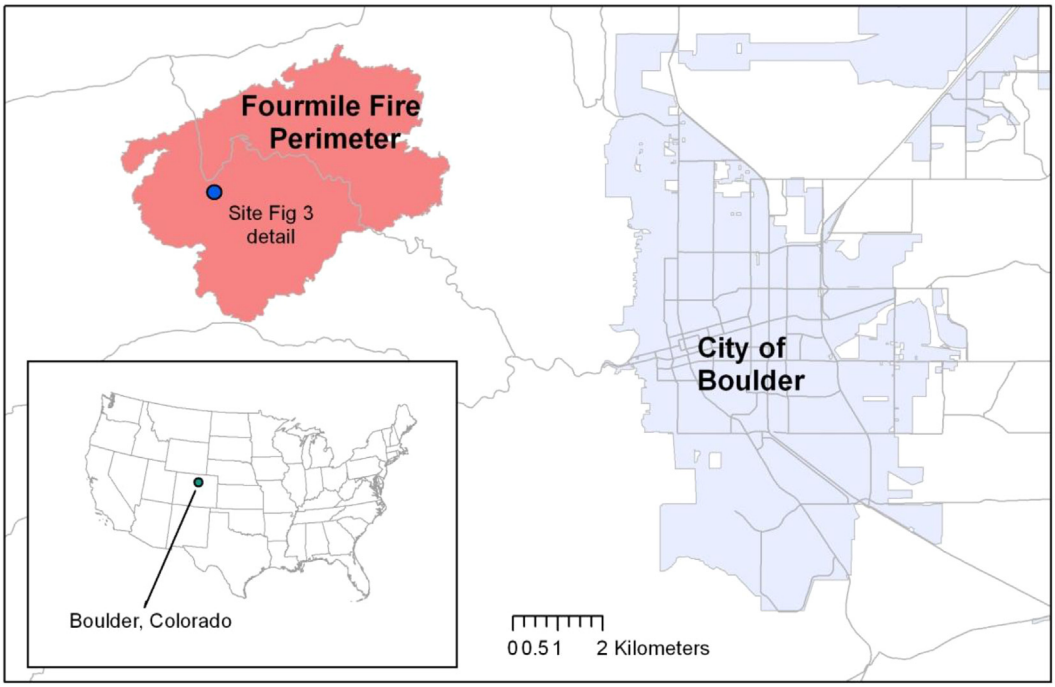

Fig. 1. Study area – the Fourmile Fire perimeter west of Boulder, Colorado.

study, information about land cover (including information about vegetation and fuels) was derived with an object-oriented image analysis (OBIA) strategy using the eCognition Developer software Trimble (2011). OBIA uses both spectral and contextual data extracted from remotely sensed imagery to create meaningful objects at multiple scales (Blaschke, 2010). A typical pixel-based study uses supervised classification to classify each pixel into discrete classes (trees, grass, etc.) based on the spectral response compared to a training sample. In contrast, in an OBIA study, imagery is first segmented into homogeneous objects and then classified based on spectral response but also geometry and contextual factors such as the relationship with neighboring objects, sub-objects, or super-objects. Many studies have found that OBIA yields higher classification accuracy than pixel-based methods for land cover classification and change detection (Bhaskaran, Paramandanda, & Ramnarayan, 2010; Blaschke, 2010; Platt & Rapoza, 2008). OBIA techniques are also able to be used to accurately distinguish areas affected by surface and crown fire (Mitri & Gitas, 2006) in ways that are transferable to other sites (Polychronaki & Gitas, 2012).

The datasets used for the OBIA classification were WorldView-2 Imagery and LiDAR data (Table 1). Land cover and vegetation classifications that use LiDAR (Mutlu, Popescu, & Zhao, 2008) or a combination of LiDAR and high spectral resolution imagery (Koetz, Morsdorf, Van Der Linden, Curt, & Allgöwer, 2008) can yield improved classifications for fire management. In this case, LiDAR and several bands unique to the WV-2 sensor (coastal blue, yellow, red edge and a second infrared band) were used to classify burned and unburned objects. Studies in the gray literature have shown that these 'special bands' can improve classification of forest species (Omar, 2010) and agricultural vegetation classes (Ruiz, Hormosilla, Serisa, Recio, & Fernandez-Sarria, 2010). Furthermore, they allow the use of NDVI-like image ratios that are potentially sensitive to differences in water and soil (Wolf, 2010). In this study, the additional bands are potentially useful for distinguishing burned from unburned areas. It should be noted that most of the studies demonstrating the superiority of WV-2 imagery were part of a contest sponsored by GeoEye (now Digitalglobe), the maker of the satellite. Additional peer reviewed studies are needed to confirm the benefits of the extra bands.

OBIA has two primary steps: segmentation and classification. To segment the images, first contrast split segmentation was applied to a 1 m slope raster to create objects that align with steep slopes (segmentation parameters: step size = 20). This segmentation procedure ensured that features with steep slopes (e.g. structures, trees, rock outcroppings) are placed in separate objects from spectrally similar neighbors. Next, a multi-resolution segmentation procedure was then applied based on WV-2 3-band RGB imagery from June 2010 (segmentation parameters: shape = 0.1, compactness = 0.5, scale = 20). Objects were then classified into one of three classes (forest, bare, grass) based on variable thresholds determined through experimentation by an image analyst (Table 3). The thresholds related to three variables: elevation, NDVI, and Brightness. Elevation represents the elevation of the object above bare earth (as derived from LiDAR), NDVI is the Normalized Difference Vegetation Index, and RBG Brightness is the average brightness across the red, green, and blue bands. The bare category includes all vegetation-free surfaces including rock outcroppings, structures, and roads. Objects with shrubs over 2 m in height (as derived from LiDAR) are included in the forest category while less than 2 m tall are included with grass.

Based on the classification, the following metrics were calculated: percent cover, forest contiguity, and proximity of canopy to structure (Table 2). In addition, 'Predominance of ladder fuels' was calculated using LiDAR data, which is associated with the quantity of branches and leaves close to the ground that create vertical

Table 3
Classification rules for pre-fire land cover.

	Elevation (m)	NDVI	Brightness (DNs)
Forest	≥2	≥0.1	<60
Bare	<2	<0.05	≥60
Grass	<2	≥0.05	–

continuity between the forest understory and the canopy. A common recommendation to homeowners is that ladder fuels should be removed (National Fire Protection Agency, 2008), e.g. up to 3 m high for trees at least 10 m tall (Slack, 2000). To calculate this variable, first the elevation of each LiDAR point was subtracted from a bare-earth elevation raster. This gave an elevation value for each point above the surface of the ground. Secondly, all returns for areas where the maximum return was <6 m were filtered out. This eliminated non-forest areas and areas with only shrubs and smaller trees. Third, the total number of returns from 1 to 3 m above the bare earth surface was divided by the total number of returns. This LiDAR metric is associated with vertical forest structure, and directly corresponds to understory biomass contained in ladder fuels (Skowronski, Clark, Nelson, Hom, & Patterson, 2007). Note that returns from 1 to 3 m in forested areas primarily indicate ladder fuels, but also can also indicate other small raised features such as understory shrubs, wildlife, or log piles. Returns between 0 and 1 m were discarded as many were ground returns that had not been filtered out due to limitations to the bare earth raster.

HIZ metrics: burned area

A second segmentation and classification was used to identify forest and grass burned by the Fourmile Fire. First, all adjacent objects with an identical classification (Forest, Bare, or Grass) were merged. A multi-resolution segmentation procedure was then applied based on post-fire WV-2 3-band RGB imagery from September 2010 (segmentation parameters: shape = 0.1, compactness = 0.5, scale = 20). Samples of grass objects (burned and unburned) and forest objects (burned and unburned) were identified (5–10 object samples for each category). For each object, the mean spectral value (pre-fire, post-fire, and change) were calculated for the 8 WorldView-2 bands, plus the following ratio indices developed specifically for WorldView-2 (Wolf, 2010):

- Normalized Difference Vegetation Index (NDVI): (NIR1 − Red)/(NIR1 + Red)
- Normalized Difference Water Index (NDWI): (Coastal − NIR2)/(Coastal + NIR2)
- Non-Homogenous Feature Difference (NHFD): (Red Edge − Coastal)/(Red Edge + Coastal)
- Normalized Difference Soil Index (NDSI): (Green − Yellow)/(Green + Yellow)

Feature space optimization (FSO), which identifies the combination of variables that yield the largest average minimum distance between samples of the different classes, was then applied. Using FSO, the following bands and indices were found to best distinguish the burned from unburned objects:

- Near-IR1 and Near-IR2 (pre-fire image)
- NDWI and NHFD (post-fire image)
- dNDWI and dNHFD (change in indices)

Based on the bands and indices above, a nearest neighborhood classification was used to classify grass and forest objects as burned or unburned. After the nearest neighbor classification, certain objects were re-classified as 'ambiguous'. Ambiguous objects are those that meet the following characteristics: (1) they were classified as forest or grass in the pre-fire image, (2) they have a brightness of <50 DNs (i.e. are in shadow) in the post-fire image, and (3) they are adjacent to burned objects. Objects that met the first two characteristics but were not adjacent to burned objects were classified as unburned.

Two additional metrics were then calculated: percent burned cover and structure survival (Table 2). Percent burned cover was simply calculated as the percentage of each HIZ comprising burned grass or forest. Structure survival was calculated in SPSS using logistic regression, a probabilistic generalized linear model for predicting the outcome of a binary state (Agresti, 2002). Logistic regression was used because it performed better than nearest neighbor classification for classifying each structure within the burn perimeter as 'survived' or 'destroyed'. The independent variables were reflectance in WorldView-2 spectral bands for both time periods; the ratios (NDWI, NHFD) for both time periods; dNDWI; dNHFD; percent grass, bare, and forest cover; and percent burned cover within the HIZ.

HIZ metrics: topography

The slope, northness, and presence of potentially hazardous landform classes were calculated across the burn perimeter and within the HIZ. Fire spreads more quickly on steep slopes, and fuels tend to be drier on south-facing slopes (in the northern hemisphere). For this reason, wildfire hazard is associated with both slope and aspect. Average slope and average northness were calculated within the HIZ of each structure. 'Northness' was defined as the average cosine of the aspect within the HIZ. Values close to one suggest a north facing slope, while values close to negative one suggest a south facing slope.

Landform classes such as canyons, ridges, saddles, and can also intensify fires. Canyons can concentrate winds, leading to increasing wildfire intensity and rate of spread. Ridges are characterized by high winds because they are higher than their surroundings. As the wind crosses the ridge it may even create a leeward eddy that exposes structures to wind and fire from the opposite direction (Federal Emergency Management Agency, 2008; Slack, 2000). Saddles are created where valleys cross ridges, and are desirable because they provide flat building surfaces and shelter. Like canyons and ridges, saddles experience high winds and fire intensity. Potentially hazardous landform classes were identified using the Topographic Position Index (TPI, Jenness, 2006). The TPI is the difference between the elevation of a grid cell and the average elevation within a neighborhood surrounding the grid cell. High TPI indicates a cell is higher than its surroundings, while a low TPI indicates that the cell is lower than its surroundings. To identify landforms, TPI was calculated using a radius of 100 m (local neighborhood) and 1 km (regional neighborhood). TPI values were then transformed by subtracting the mean value and dividing by the standard deviation (the standard deviation was 11 m in the case of TPI-100 m and 81 m in the case of TPI-1 km). Canyons, ridges, and saddles were classified based on the two TPI *z*-scores and slope (Table 4, adapted from Jenness, 2006).

Fires typically travel upslope, thus structures whose widest sides face downhill are more exposed to the probable fire path than those whose narrowest sides face downhill (Federal Emergency Management Agency, 2008; Slack, 2000). Also, larger structures have greater exposure than smaller ones. Exposure was measured using the aspect ratio (length-to-width) of the building footprint polygon on its downhill-facing side. For example, an exposure value of 2 means that a structure is twice as long in the downhill-facing direction from which the fire is likely to come, as it is in the direction perpendicular to downhill. The downhill-facing direction was determined by (1) generating an aspect raster from a 1 m DEM, (2) creating cosine and sine rasters from the aspect raster, (3) calculating the zonal mean of sine and cosine within the *HIZ* and (4) using the arctan2 function to convert the zonal mean sine and cosine into an 'average aspect' raster. The minimum bounding geometry length and width were then calculated for each structure

Table 4
Classification rules for landform class using the topographic position index (TPI). "More hazardous" landform classes are shown in bold.

TPI-100 m (standard deviations from the mean)				
		<−1	−1 to 1	>1
TPI-1 km (standard deviations from the mean)	>1	**Saddle**	Flat ridge or mesa tops	**Ridge**
	−1 to 1	**Chimney**	Flat slope	Drainage divide
	<−1	**Canyon**	Valley bottom	Local high point within valley

with respect to the 'average aspect' (i.e. dominant downhill direction). For each topography variable, the median value within the HIZ was compared to the median value within fire perimeter as a whole.

Accuracy assessment

The object-oriented classification of pre-fire land cover, and burned area was validated on a manual interpretation of 600 objects. Of the 600 objects, 200 were randomly selected from anywhere within the burn perimeter, 204 objects were randomly selected from within the HIZ, and 196 objects were "ground truthed" in the field. Two image analysts visually classified the 404 randomly selected objects based primarily on the true-color WV-2 imagery. In cases where the class was not obvious, or when the classification by the two analysts differed, the analysts used supplemental imagery such as a color-infrared composite of the WV-2 imagery or imagery from various dates from Google Earth to make the class determination. An additional 196 objects were visited in the field in August 2011, 11 months after the fire. During this "windshield survey" object classifications were evaluated at safe stopping points along the public roads within the burn perimeter. Following Pontius and Millones (2011), the accuracy of the object classification was evaluated with using the following metrics: total agreement, allocation disagreement, quantity disagreement, and commission intensity. Total agreement is the objects correctly classified divided by the total objects, weighted by each object class's prevalence in the overall landscape (determined by the random sample of the burn perimeter). Quantity disagreement is the percentage of classification errors caused by an incorrect prediction in the proportions of the classes (Pontius & Millones, 2011). Allocation disagreement is the percentage of classification errors caused by an incorrect prediction in the location of particular classes. Commission intensity describes the percentage of classification errors where an object is predicted to be a particular class when in fact it is a different class. Omission intensity describes the percentage of classification errors where an object of a particular class is classified as something else. 'Structure survival' was validated separately using data on structure survival collected by Boulder County, and accuracy was assessed using the Pontius & Millones, 2011 method.

Characterizing hazard in the HIZ

For the study area, the average value of metrics for the HIZ and, for comparison, those of the fire perimeter as a whole (the WUI) were reported. The values of HIZ metrics for individual structures, while of interest to homeowners, are not reported here.

In addition, a simple HIZ hazard index was created from 8 metrics. To do this, each pre-fire variable in Table 2 was re-classified into a binary variable ("more hazardous" and "less hazardous"). For continuous variables (percent non-bare cover, forest contiguity, predominance of ladder fuels, slope, northness, exposure), "more hazardous" was defined as a value in the top quintile of all structures. For landform class, a HIZ was classified "more hazardous" if it was characterized as canyon, ridge top, saddle, or chimney. For adjacency of canopy to structure, any HIZ with a forest canopy adjoining or intersecting a structure was "more hazardous". The number of times a HIZ had an attribute classified as "more hazardous" was then summed, providing a simple index (0–8).

The HIZ hazard index can be used to identify individual structures that may be hazardous, but also clusters (i.e. neighborhoods) of high and low hazard. To identify such clusters, Local Moran's I (Anselin, 1995) was calculated and mapped using OpenGeoDa (Anselin, Syabri, & Kho, 2006). Local Moran's I identifies observations that are significantly autocorrelated to neighboring observations. Positive autocorrelation suggests that HIZes have similar values to nearby HIZes in terms of their hazard index (i.e. high values are next to other high values or low values are next to other low values). Negative autocorrelation suggests that HIZes have dissimilar values to nearby HIZes. In this case, an inverse distance weighing function was used to construct the spatial weights matrix, and a spatially random reference was used to assess statistical significance ($p = 0.01$ level).

Results

Accuracy assessment

The classification accuracies of pre-fire land cover (89% total agreement) and burn area (90% total agreement) were high overall (Table 5). Furthermore, most of the classification errors were due to allocation disagreement rather than quantity disagreement. In terms of individual classes, bare had slightly higher errors of omission and commission than forest or grass, most likely because bare overlaps spectrally and elevation-wise with dry grass interspersed with rocky soil (Table 6a). The most common error in the burn area classification was classifying a burned object as not burned (16% error of omission, Table 6b). This could occur in objects that are partially burned but retain photosynthetic activity (high NDVI) to which the classifier is sensitive. Overall, however, the classification accuracies for individual classes were high.

The classification accuracy of structure survival was also high (88% total agreement; area under the curve of .92). The percentage of burned area and the amount of pre-fire forest are helpful for classifying structure survival (Table 7). This suggests that, not surprisingly, the more land in the HIZ burns, the more likely a structure is destroyed. However, the errors of commission for structure survival were high at 32% (Table 6c), indicating that the model overpredicted destroyed structures. Indeed, many structures survived the fire despite having a high proportion of forest and high proportion of burned land cover, potentially due to structure characteristics. Surprisingly, spectral information (WorldView-2 bands and related indices) was not useful in classifying structure survival. No post-fire LiDAR data exists, which could have been potentially used to create more accurate classifications of structure survival. Since structure survival could not be directly classified, only inferred from the extent of pre-fire forest and burning in the HIZ, this is

Table 5
Classification accuracy summary of pre-fire land cover, burn area, and structure survival.

	Pre-fire land cover	Burn area	Structure survival
Total agreement	89	90	88
Allocation disagreement	9	10	8
Quantity disagreement	2	<1	4

Table 6
Confusion matrices of pre-fire land cover, burn area, and structure survival.

A. Pre-fire land cover

		Visual interpretation				Total	Errors of commission
		Other	Bare	Forest	Grass		
Nearest neighbor classification	Bare	1	51	3	7	62	18%
	Forest	0	0	233	28	261	11%
	Grass	0	7	22	248	277	10%
	Total	1	58	258	283	600	
Errors of omission			12%	10%	12%		

B. Burn area

		Visual interpretation		Total	Errors of commission
		Not burned	Burned		
Nearest neighbor classification	Not burned	286	44	346	13%
	Burned	22	232	254	9%
	Ambiguous	16	0	0	
	Total	323	276	600	
Errors of omission		12%	16%		

C. Structure survival

		Ground truth		Total	Errors of commission
		Survived	Destroyed		
Logistic regression classification	Survived	479	27	506	5%
	Destroyed	56	118	174	32%
	Total	535	145	600	
Errors of omission		10%	19%		

not a widely applicable model despite the high classification accuracy.

HIZ metrics

Given the high accuracy of pre-fire land cover and burning, object classifications can be evaluated with some confidence. First, the average characteristics of the HIZ were compared to the fire perimeter as a whole (the WUI). Pre-fire, 47% of the WUI comprised forest, 45% comprised grass, and 7% comprised bare (Table 8). In contrast, the HIZ had a higher percentage of bare (15%) and a lower percentage of forest (37%) than the WUI in the fire perimeter. The forest contiguity (as measured by the average distance between the edges of forest objects) was found to be lower within the HIZ than within the WUI (2 m vs. 1 m). The predominance of ladder fuels (as measured by the percentage of first returns from 1 to 3 m) was similar within the WUI and the HIZ (11% vs. 9%). While 55% of the area within the WUI burned, only 34% burned within the HIZ. In short, the average HIZ of Fourmile Canyon are actually less hazardous than the WUI within the fire perimeter according to several of our metrics – it contain more bare and less forest land, have more widely spaced canopies, and experienced less extensive burning potentially due to fire suppression.

In terms of topography, the WUI has a greater percentage of land with steep slope (>20°) than does the HIZ (54% vs. 29%, Table 8). In contrast, the HIZ has a slightly greater percentage of land classified as canyons than does the WUI (13% vs. 5%). This is not surprising, as access and construction is more difficult in steep or inaccessible terrain, and major roads tend to follow canyons. Ridges, chimneys, and saddles constitute a small percentage of the WUI and a similarly small percentage of the HIZ. The 'northness' of the HIZ indicates that the WUI on average tilts farther southward by 8° compared to the HIZ. Overall sites selected for structures tend to be a little less steep and are slightly less southward facing than the WUI, but otherwise the topography is similar.

Table 7
Results of logistic regression classification of structure survival.

	B	S.E.	Wald	df	Sig.	Exp(*B*)
Pre-fire Forest (m^2)	.002	.000	69.706	1	.000	1.002
Percent Burned	7.054	.585	145.409	1	.000	1156.969
Constant	−6.060	.516	137.798	1	.000	.002

Table 8
Average metrics of HIZ compared to fire perimeter (WUI).

		HIZ	WUI
Pre-fire Land Cover	Bare	15%	7%
	Forest	37%	47%
	Grass	43%	45%
	Forest contiguity (m)	2	1
	Predominance of ladder fuels	9%	11%
Burn Area	Forest burned	9%	22%
	Grass burned	25%	33%
	Ambiguous	3%	2%
	Unburned/bare	63%	42%
Topography	Ridge	5%	4%
	Canyon	13%	5%
	Chimney	4%	8%
	Saddle	<1%	<1%
	>20° slope	29%	55%
	Other	55%	39%

HIZ hazard index

Out of 1322 structures within the fire perimeter, 81% score as "more hazardous" on only 1–3 of the 8 metrics. An additional 7% of structures did not score as "more hazardous" on any metrics, while 11% scored as "more hazardous" on 4 or more metrics (Fig. 2).

The Local Moran's I map (each point representing a HIZ) shows while most HIZes do not demonstrate significant local spatial autocorrelation, there are several clusters of significant spatial autocorrelation (Fig. 3). Of particular interest, there are high–high clusters at the center of the burn perimeter running along canyon roads, in particular parts of Fourmile Canyon Canyon Drive and Gold Run Road. HIZes in this area tend to score high in the hazard index due to the steep slopes, narrow canyon topography, and contiguous forest canopy. There are also several areas with low–low clusters, including within the town of Gold Hill and in the northeastern portion of the burn perimeter along Sunshine Canyon Road. These areas tended to have more bare land cover, spread-out tree canopies, and lower slope. In short, while the HIZ hazard index is highly spatially heterogeneous, there are some clusters of high or low hazard index values.

The HIZ hazard index can also be used to assess or identify individual HIZes. To illustrate, two HIZes are shown, one with a score of 5 (Fig. 4A) and one with a score of 6 (Fig. 4B). Fig. 4A shows a HIZ that was rated "more hazardous" in terms of: percentage of non-bare land cover (95%), adjacency of canopy to structure, predominance of ladder fuels (18% of first returns from 1 to 3 m), northness (faces due south), and landform class (ridge). The grass and forest were almost entirely burned, and the structure was destroyed in the fire. Fig. 4B shows a HIZ that was rated "more hazardous" in terms of: forest contiguity (average nearest neighbor distance of zero), slope (average of 25°), landform class (canyon), and exposure (the long side of the house is facing northeast, which is the downslope direction as well as the direction from which the fire came). Though the fire burned forest right up to the structure, the structure was not destroyed in the fire.

Conclusion

A suite of methods was presented that is designed to extract specific information about the HIZ and the wider landscape. The

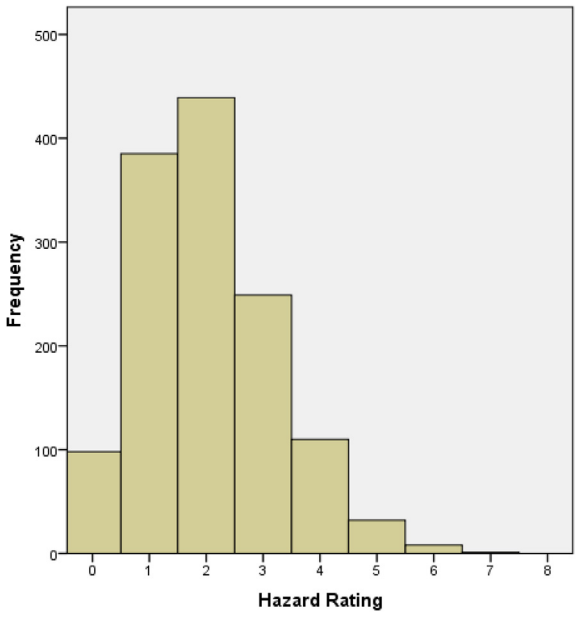

Fig. 2. Frequency distribution of HIZ Hazard Index. The index is calculated for each HIZ and represents the number of metrics classified as 'more hazardous' (0–8).

methods go beyond previous GIS approaches which typically operate at relatively course spatial resolutions and focus on the WUI as a whole rather than the HIZ. In contrast, the methods in this study have numerous advantages. First, the data sources have very high spatial and spectral resolution (0.5 m RGB, 2 m 8-band multispectral, and 1 m LiDAR) that allow fine-scale variation in HIZ to be characterized. Secondly, the object-oriented classification approach yields high classification accuracy and can easily integrate topological relationships (i.e. adjacency of canopy to structure, forest contiguity). Third, measures of topography (for example, northness, TPI, forest contiguity, predominance of ladder fuels) provided information that relate to standards for ignition reduction (e.g. Federal Emergency Management Agency, 2008).

The suite of methods was applied to the Fourmile Canyon fire perimeter. Compared to the WUI, the HIZ is characterized by a greater percentage of grass and bare land, and lower percentage forest; a greater percentage of canyons and a lower percentage of steep slopes (>20°); less south-facing aspect; and a lower percentage of burned land, especially forest. The findings are consistent with the findings of Graham et al. (2012, 110 pp.) which found that much of the structure destruction was caused by ground fire and that there was a strong topographic effect whereby canyons were less exposed to fire. This is also consistent with studies that suggest that roads and bare ground in the HIZ actually reduce fire intensity (Cohen & Stratton, 2008). While the logistic regression classification of structure survival produced too many 'false positives' to be useful, it did reveal an association between pre-fire forest cover and structure survival. The result is consistent with empirical studies of previous fires that show the proximity and amount of trees near structures relate to structure survival (Bhandary & Muller, 2009; Gibbons et al., 2012). The HIZ hazard index was spatially heterogeneous, but with several clusters of high and low index values. The town of Gold Hill was one 'low–low' cluster, which is consistent studies that show the probability of housing loss is lower in areas of highest housing density and fewer number of isolated development clusters (Syphard, Bar Massada, Butsic, & Keeley, 2013).

Not only are the results consistent with the literature on structure survival, they are also of practical use and can be broadly applied to other fire-prone areas. The methods can be easily used to identify specific structures that with potentially hazardous HIZes. Structures that are 'flagged' through this process could be followed up with site visits or automatic mailings. The outputs could also be used in comprehensive hazard assessments for structures such as Wildfire Wizard or the National Fire Protection Agency structure assessment rating form (National Fire Protection Agency, 2008).

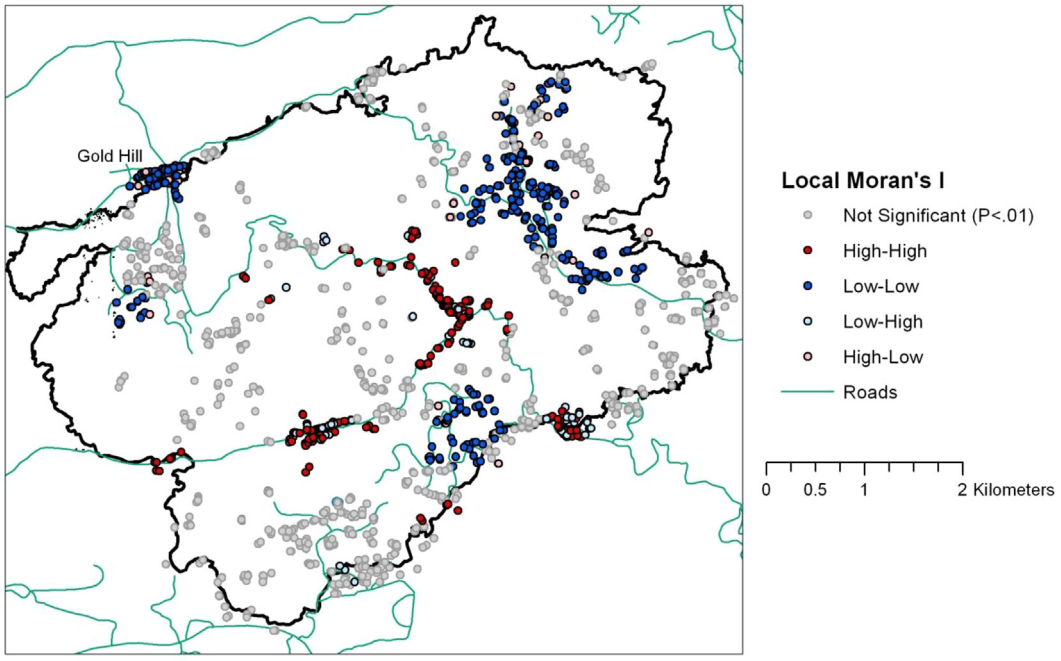

Fig. 3. Local Moran's I of HIZ Hazard Index within the Fourmile Fire Perimeter. 'High–high' represents clusters of HIZes with high HIZ Hazard Index values; 'low–low' represents clusters of HIZes with low HIZ Hazard Index values; 'not significant' represents areas where the HIZ Hazard Index values are not related to neighboring values.

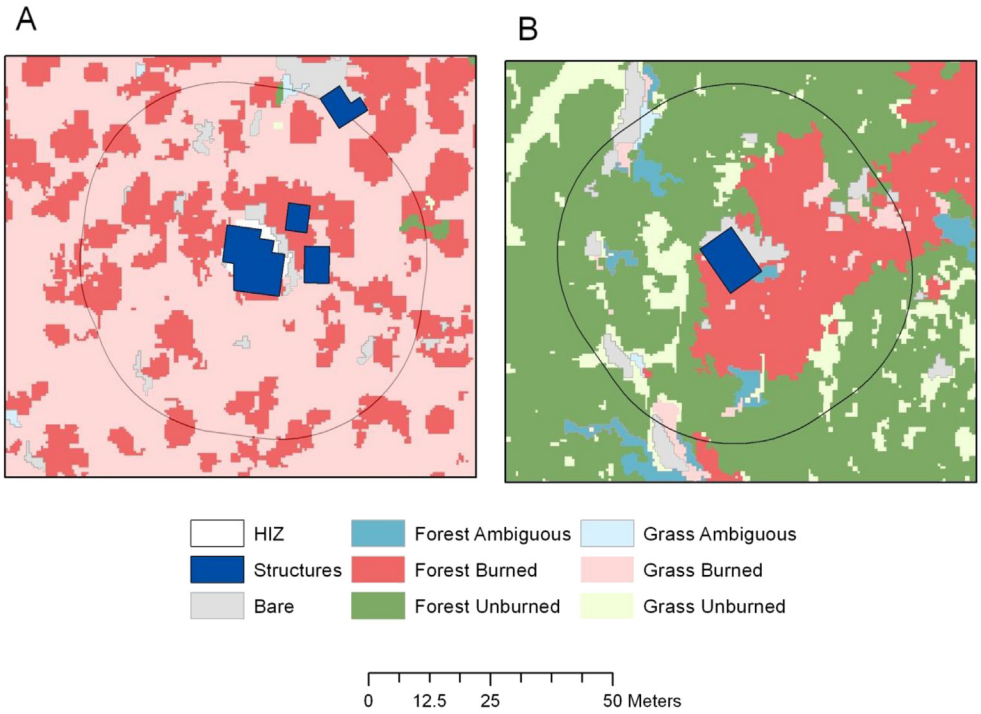

Fig. 4. Examples of HIZes with high HIZ Hazard Index values (location within study area shown in Fig. 1). A shows an area rated "more hazardous" in terms of percentage of non-bare land cover, adjacency of canopy to structure, predominance of ladder fuels, northness, and landform class. B shows an area that was rated "more hazardous" in terms of forest contiguity, slope, landform class, and exposure.

Furthermore, such information along with *in situ* data could be used to help design or refine Community Wildlife Protection Plans (CWPP, Jakes et al., 2011), which identify high priority areas for hazardous fuel reduction, and make recommendations for ways homeowners can reduce structure ignitability. This would particularly benefit rural communities, which typically focus on post-disaster recovery and response rather than mitigation in their planning process (Frazier, Walker, Kumari, & Thompson, 2013). Unfortunately, while the methods described here have great promise, availability of LiDAR and multispectral VHR satellite imagery remains expensive and limited. Furthermore, object-oriented image analysis requires expertise and software that is not available in most planning offices. Nevertheless, the methods described in this study show great promise in helping to evaluate characteristics of the HIZ pre- and post-fire.

Acknowledgements

I would like to thank Matthew Toich and Julie Ivers, Gettysburg College class of 2012, for their work on this project. I would also like to thank the following data providers: Digitalglobe for generously providing the WorldView-2 Data, Boulder County for making building footprints available to the public, and Boulder Creek Critical Zone Observatory for the LiDAR point clouds. I would also like to thank Gettysburg College for providing critical funding for this project through a Provost Research and Professional Development Grant.

References

Ager, A. A., Vaillant, N. M., & Finney, M. A. (2010). A comparison of landscape fuel treatment strategies to mitigate wildland fire risk in the urban interface and preserve old forest structure. *Forest Ecology and Management, 259*(8), 1556–1570.

Agresti, A. (2002). *Categorical data analysis*. New York: Wiley-Interscience.

Anselin, L. (1995). Local Indicators of Spatial Association – LISA. *Geographical Analysis, 27*(2), 93–115.

Anselin, L., Syabri, I., & Kho, Y. (2006). GeoDa: an introduction to spatial data analysis. *Geographical Analysis, 38*(1), 5–22.

Badia, A., Serra, P., & Modugno, S. (2011). Identifying dynamics of fire ignition probabilities in two representative Mediterranean wildland–urban interface areas. *Applied Geography, 31*, 930–940.

Bar Massada, A., Radeloff, V. C., Stewart, S. I., & Hawbaker, T. J. (2009). Wildfire risk in the wildland–urban interface: a simulation study in northwestern Wisconsin. *Forest Ecology and Management, 258*(9), 1990–1999.

Beverly, J. L., Bothwell, P., Conner, J. C. R., & Herd, E. P. K. (2010). Assessing the exposure of the built environment to potential ignition sources generated from vegetative fuel. *International Journal of Wildland Fire, 19*, 299–313.

Bhandary, U., & Muller, B. (2009). Land use planning and wildfire risk mitigation: an analysis of wildfire-burned subdivisions using high-resolution remote sensing imagery and GIS data. *Journal of Environmental Planning and Management, 52*(7), 939–955.

Bhaskaran, S., Paramandanda, S., & Ramnarayan, M. (2010). Per-pixel and object-oriented classification methods for mapping urban features using Ikonos satellite data. *Applied Geography, 30*, 650–665.

Blaschke, T. (2010). Object based image analysis for remote sensing. *ISPRS Journal of Photogrammetry and Remote Sensing, 65*, 2–16.

Castillo, M. (2012). The identification and assessment of areas at risk of forest fire using fuzzy methodology. *Applied Geography, 35*, 199–207.

Chas-Amil, M. L., Touza, J., & Garcia-Martinez, E. (2013). Forest fires in the wildland–urban interface: a spatial analysis of forest fragmentation and human impacts. *Applied Geography, 43*, 127–137.

Cohen, J. D. (2000). Preventing disaster: home ignitability in the wildland–urban interface. *Journal of Forestry, 98*(3), 15–21.

Cohen, J. D. (2001). Wildland–urban fire—a different approach. In *Proceedings of the Firefighter Safety Summit, Nov. 6–8, 2001, Missoula, MT*. Fairfax, VA: International Association of Wildland Fire.

Cohen, J. D. (2008). The wildland–urban interface fire problem: a consequence of the fire exclusion paradigm. *Forest History Today Fall*, 20–26.

Cohen, J. D. (1991). *A site-specific approach for assessing the fire risk to structures at the wildland/urban interface*. Missoula, MT: Missoula Fire Sciences Lab. www.firelab.org.

Cohen, J. D., & Butler, B. W. (1998). *Modeling potential structure ignitions from flame radiation exposure with implications for wildland/urban interface fire management*. USDA Forest Service, Intermountain Research Station, Missoula, MT: Intermountain Fire Sciences Laboratory.

Cohen, J. D., & Stratton, R. D. (2008). *Home destruction examination: Grass Valley Fire, Lake Arrowhead, California. U.S.*. Department of Agriculture, Forest Service, Pacific Southwest Region (Region 5). Tech. Paper R5-TP-026b. (Vallejo, CA).

Federal Emergency Management Agency. (2008). *Home builder's guide to construction in wildfire zones*. Technical Fact Sheet No. 4 – Defensible Space. Retrieved from http://www.fema.gov/library/viewRecord.do?id=3646. Last Accessed 08.06.13.

Frazier, T. G., Walker, M. H., Kumari, A., & Thompson, C. M. (2013). Opportunities and constraints to hazard mitigation planning. *Applied Geography, 40*, 52–60.

Gibbons, P., Van Bommel, L., Gill, A. M., Cary, G. J., Driscoll, D. A., Bradstock, R. A., et al. (2012). Land management practices associated with house loss in wildfires. *PLoS One, 7*(1), e29212.

Graham, R., Finney, M., McHugh, C., Cohen, J., Calkin, D., Stratton, R., et al. (2012). *Fourmile Canyon Fire Findings*. Gen. Tech. Rep. RMRS-GTR-289. Fort Collins, CO: US Department of Agriculture, Forest Service, Rocky Mountain Research Station.

Guglietta, D., Conedera, M., Mazzoleni, S., & Ricotta, C. (2011). Mapping fire ignition risk in a complex anthropogenic landscape. *Remote Sensing Letters, 2*(3), 213–219.

Hammer, R. B., Stewart, S. I., & Radeloff, V. C. (2009). Demographic trends, the wildland–urban interface, and wildfire management. *Society and Natural Resources, 22*, 777–782.

Herrero-Corral, G., Jappiot, M., Bouillon, C., & Long-Fournel, M. (2012). Application of a geographical assessment method for the characterization of wildland–urban interfaces in the context of wildfire prevention: a case study in western Madrid. *Applied Geography, 35*(1), 60–70.

Holden, Z. A., & Jolly, W. M. (2011). Modeling topographic influences on fuel moisture and fire danger in complex terrain to improve wildland fire management decision support. *Forest Ecology and Management, 262*, 2133–2141.

Jakes, P. J., Nelson, K. C., Enzler, S. A., Burns, S., Cheng, A. S., Sturtevant, V., et al. (2011). Community wildfire protection planning: is the Healthy Forests Restoration Act's vagueness genius? *International Journal of Wildland Fire, 20*(3), 350–363.

Jenness, J. (2006). *Topographic Position Index (tpi_jen.avx) extension for ArcView 3.x, v. 1.3a*. Jenness Enterprises. Retrieved from http://www.jennessent.com/arcview/tpi.htm. Last Accessed 08.06.13.

Koetz, B., Morsdorf, F., Van Der Linden, S., Curt, T., & Allgöwer, B. (2008). Multi-source land cover classification for forest fire management based on imaging spectrometry and LiDAR data. *Forest Ecology and Management, 256*(3), 263–271.

Lampin-Maillet, C., Long-Fournel, M., Ganteaume, A., Jappiot, M., & Ferrier, J. P. (2011). Land cover analysis in wildland–urban interfaces according to wildfire risk: a case study in the south of France. *Forest Ecology and Management, 261*(12), 2200–2213.

Lein, J. K., & Stump, N. I. (2009). Assessing wildfire potential within the wildland–urban interface: a southeastern Ohio example. *Applied Geography, 29*, 21–34.

Maranghides, A., & Mell, W. (2009). *A case study of a community affected by the Witch and Guejito fires*. National Institute of Standards and Technology Technical Note 1635.

Mell, W. E., Manzello, S. L., Maranghides, A., Butry, D. T., & Rehm, R. G. (2010). The wildland–urban interface fire problem – current approaches and research needs. *International Journal of Wildland Fire, 19*, 238–251.

Mitri, G. H., & Gitas, I. Z. (2006). Fire type mapping using object-based classification of Ikonos imagery. *International Journal of Wildland Fire, 15*(4), 457–462.

Montz, B. E., & Tobin, G. A. (2011). Natural hazards: an evolving tradition in applied geography. *Applied Geography, 31*, 1–4.

Mutlu, M., Popescu, S., & Zhao, K. (2008). Sensitivity analysis of fire behavior modeling with LIDAR-derived surface fuel maps. *Forest Ecology and Management, 256*, 289–294.

Narayanaraj, G., & Wimberly, M. C. (2012). Influences of forest roads on the spatial patterns of human- and lightning-caused wildfire ignitions. *Applied Geography, 32*, 878–888.

National Fire Protection Agency (NFPA) 1144. (2008). *Standard for reducing structure ignition hazards from wildland fire*.

National Interagency Fire Center (NIFC). (2009). *Quadrennial fire review final report, January 2009*. Retrieved from http://www.nifc.gov/QFR/QFR2009Final.pdf. Last Accessed 08.06.13.

National Interagency Fire Center (NIFC). (2012). *National year-to-date report on fires and acres burned by state*. Retrieved from http://www.nifc.gov/fireInfo/fireInfo_stats_YTD2012.html. Last accessed 08.06.13.

Omar, H. (2010). Commercial timber tree species identification using multispectral Worldview-2 Data. In *WorldView-2 8-Bands Research Challenge* (pp. 2–13).

Ottmar, R. D., Blake, J. I., & Crolly, W. T. (2012). Using fine-scale fuel measurements to assess wildland fuels, potential fire behavior and hazard mitigation treatments in the southeastern USA. *Forest Ecology and Management, 273*, 1–3.

Platt, R. V. (2010). The wildland–urban interface: evaluating the definition effect. *Journal of Forestry, 108*(1), 9–15.

Platt, R. V., & Rapoza, L. M. (2008). An evaluation of an object-oriented paradigm for land use/land cover classification. *Professional Geographer, 60*(1), 87–100.

Polychronaki, A., & Gitas, I. Z. (2012). Burned area mapping in Greece using SPOT-4 HRVIR images and object-based image analysis. *Remote Sensing, 4*, 424–438.

Pontius, R. G., & Millones, M. (2011). Death to Kappa: birth of quantity disagreement and allocation disagreement for accuracy assessment. *International Journal of Remote Sensing, 32*(15), 4407–4429.

Radeloff, V. C., Hammer, R. B., Stewart, S. I., Fried, J. S., Holcomb, S. S., & McKeefry, J. F. (2005). The wildland–urban interface in the United States. *Ecological Applications, 15*(3), 799–805.

Ruiz, L. A., Hormosilla, T., Serisa, G., Recio, J. A., & Fernandez-Sarria, A. (2010). A multi-approach and object-oriented strategy for updating LU/LC Geodatabases based on WorldView-2 Imagery. In *WorldView-2 8-Bands Research Challenge*.

Skowronski, N., Clark, K., Nelson, R., Hom, J., & Patterson, M. (2007). Remotely sensed measurements of forest structure and fuel loads in the pinelands of New Jersey. *Remote Sensing of Environment, 108*, 123–129.

Slack, P. (2000). *Firewise construction: Design and materials*. Colorado State Forest Service and the Federal Emergency Management Agency. Retrieved from http://csfs.colostate.edu/pdfs/construction_booklet.pdf. Last Accessed 08.06.13.

Syphard, A. D., Bar Massada, A., Butsic, V., & Keeley, J. E. (2013). Land use planning and wildfire: development policies influence future probability of housing loss. *PLOS One, 8*(8), e71708.

Syphard, A., Keeley, J., Bar Massada, A., Brennan, R., & Radeloff, V. C. (2012). Housing arrangement and location determine the likelihood of housing loss due to wildfire. *PLOS One, 7*(3), e33954.

Theobald, D. M., & Romme, W. H. (2007). Expansion of the US wildland–urban interface. *Landscape and Urban Planning, 83*(4), 340–354.

Trimble. (2011). *eCognition Developer 8.7 Reference Book*. Trimble Germany GmbH, Trappentreustr 1, D-80339. (München, Germany).

Veblen, T. T., Kitzberger, T., & Donnegan, J. (2000). Climatic and human influences on fire regimes in ponderosa pine forests in the Colorado Front Range. *Ecological Applications, 10*(4), 1178–1195.

Wolf, A. (2010). Using WorldView 2 Vis-NIR MSI Imagery to support land mapping and feature extraction using normalized difference index ratios. In *WorldView-2 8-Bands Research Challenge*.